

Frascati Physics Series Vol. VVVVVV (xxxx), pp. 000-000  
XX CONFERENCE – Location, Date-start - Date-end, Year

## NEW MEASUREMENTS OF THE ANGLE $\gamma$ FROM THE *BABAR* EXPERIMENT

Toyoko Jennifer Orimoto

(on behalf of the *BABAR* Collaboration)

*Lawrence Berkeley National Laboratory, 1 Cyclotron Road, Berkeley, CA 94720*

### Abstract

Measuring the angle  $\gamma$  is an important part of over-constraining the Unitarity Triangle to test Standard Model predictions. There are a number of methods to measure  $\gamma$ , and we present results on the progress made in measuring  $\gamma$  with  $B$  meson decays, using data collected with the *BABAR* detector at the PEP-II asymmetric energy  $e^+e^-$  collider at SLAC.

### 1 Introduction

The Cabibbo-Kobayashi-Maskawa (CKM) quark flavor-mixing matrix <sup>1)</sup> provides an elegant explanation of the origin of  $CP$  violation within the Standard Model of particle interactions.  $CP$  violation manifests itself as a non-zero area of the Unitarity Triangle of the CKM matrix <sup>2)</sup>. While it is sufficient to measure one of the angles to demonstrate the existence of  $CP$  violation, the

*Contributed to International Workshop On Discoveries In Flavour Physics At E+ E- Colliders,  
2/28/2006-3/3/2006, Frascati, Italy*

*Work supported in part by US Department of Energy contract DE-AC02-76SF00515*

Unitarity Triangle must be over-constrained to demonstrate that the CKM mechanism is the correct explanation of this phenomenon. We report on the latest measurements of the angle  $\gamma$  from the *BABAR* Experiment.

## 2 $\gamma$ from $B^- \rightarrow D^{(*)0} K^{(*)-}$ Decays

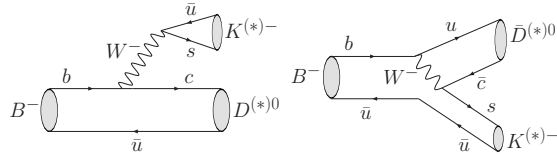


Figure 1: Feynman diagrams for CKM and color-favored  $B^- \rightarrow D^{(*)0} K^{(*)-}$  (left) and CKM and color-suppressed  $B^- \rightarrow \bar{D}^{(*)0} K^{(*)-}$  (right).

The decays  $B^- \rightarrow \tilde{D}^{(*)0} K^{(*)-}$  can be used to probe  $\gamma$  since  $b \rightarrow c\bar{u}s$  and  $b \rightarrow u\bar{c}s$  transitions have a relative weak phase of  $\gamma$ .  $\tilde{D}^0$  indicates either a  $D^0$  or  $\bar{D}^0$  meson, and “ $(*)$ ” indicates either a  $D$  or  $D^*$  meson. These decays are particularly attractive for  $CP$  studies since they are tree-level processes, which lack the theoretical uncertainties that can arise from penguin processes. Figure 1 depicts the Feynman diagrams for the color-suppressed mode  $B^- \rightarrow D^{(*)0} K^{(*)-}$  and the color-favored mode  $B^- \rightarrow \bar{D}^{(*)0} K^{(*)-}$ . The ratio of the suppressed amplitude to the favored amplitude is proportional to  $r_B^{(*)} e^{i\delta_B^{(*)}} e^{i\gamma}$ , where  $r_B^{(*)} \equiv \frac{|A(B^- \rightarrow D^{(*)0} K^{(*)-})|}{|A(B^- \rightarrow \bar{D}^{(*)0} K^{(*)-})|}$  is the ratio of the magnitudes of the suppressed and favored amplitudes,  $\delta_B^{(*)}$  is the unknown relative strong phase, and  $\gamma$  is the relative weak phase between the decays, which can be written in terms of the CKM matrix elements as  $\gamma \equiv \arg \left[ -\frac{V_{ud} V_{cb}^*}{V_{cd} V_{cb}^*} \right]$ .  $r_B^{(*)}$  is estimated to be  $\sim 0.1 - 0.3$ <sup>3)</sup>.  $r_B^{(*)}$  is a crucial parameter since it is a measure of the interference between these decays and thus indicates our sensitivity to measuring  $\gamma$ . In order to measure the phase  $\gamma$ , these decays must interfere, and this occurs when the same final state  $f$  is accessible by both the  $D^0$  and  $\bar{D}^0$ .

A number of theoretically clean methods are available for measuring  $\gamma$  from  $B^- \rightarrow \tilde{D}^{(*)0} K^{(*)-}$  decays. We report here measurements of  $\gamma$  from *BABAR* using the Gronau-London-Wyler (GLW)<sup>4)</sup>, the Atwood-Dunietz-Soni (ADS)<sup>5)</sup>, and the Giri-Grossman-Soffer-Zupan (GGSZ) Dalitz<sup>6)</sup> methods. Although these methods similarly rely on the interference of  $B$  decays into  $\tilde{D}^0 K$ , they differ in the use of the final state of the  $D$  meson.

## 2.1 $\gamma$ from the Gronau-London-Wyler Method

The GLW method exploits the relationship between the  $CP$  and flavor states of the neutral  $D$  mesons to measure  $\gamma$ . The  $CP$  even states that are used are  $\pi^+\pi^-$  and  $K^+K^-$ , while the  $CP$  odd states used are  $K_S^0\pi^0$ ,  $K_S^0\phi$ ,  $K_S^0\omega$ . The results are usually expressed in terms of the ratio of the charge-averaged partial rates  $R_{CP\pm}$  and the partial-rate charge asymmetries  $A_{CP\pm}$ , which arise from the relationships between the  $CP$  and flavor states:

$$R_{CP\pm} = \frac{\Gamma(B^- \rightarrow D_{CP\pm}^0 K^-) + \Gamma(B^+ \rightarrow D_{CP\pm}^0 K^+)}{[\Gamma(B^- \rightarrow D^0 K^-) + \Gamma(B^+ \rightarrow \bar{D}^0 K^+)]/2} \quad (1)$$

$$A_{CP\pm} = \frac{\Gamma(B^- \rightarrow D_{CP\pm}^0 K^-) - \Gamma(B^+ \rightarrow D_{CP\pm}^0 K^+)}{\Gamma(B^- \rightarrow D_{CP\pm}^0 K^-) + \Gamma(B^+ \rightarrow D_{CP\pm}^0 K^+)}, \quad (2)$$

where  $D_{CP\pm}^0 = (D^0 \pm \bar{D}^0)/\sqrt{2}$  are  $CP$  eigenstates of the neutral  $D$  mesons, written in terms of the flavor states. In the absence of  $D^0 - \bar{D}^0$  mixing<sup>7)</sup>,  $R_{CP\pm}$  and  $A_{CP\pm}$  are related to  $r_B$ ,  $\delta_B$ , and  $\gamma$  through the following relationships:

$$R_{CP\pm} = 1 + r_B^2 \pm 2r_B \cos \delta_B \cos \gamma \quad (3)$$

$$A_{CP\pm} = \pm 2r_B \sin \delta_B \sin \gamma / R_{CP\pm} \quad (4)$$

This results in three unknowns,  $r_B$ ,  $\delta_B$ , and  $\gamma$  and three independent observables, since  $A_{CP+}R_{CP+} = A_{CP-}R_{CP-}$ . In addition, this method results in a four-fold ambiguity on  $\gamma$ .

The GLW method is theoretically clean since it exploits relationships that are exact, and the hadronic uncertainties associated with the decays are small. However, this method is experimentally challenging since the branching fractions for these  $B$  and  $D$  decays are relatively small.

The latest results from the GLW analyses of  $B^\pm \rightarrow D_{CP}^0 K^{(*)\pm}$  from *BABAR*, based on a sample of 232 million  $B\bar{B}$  events, can be seen in Table 1<sup>8), 9)</sup>. The signal yields are  $131 \pm 17$   $CP$  even and  $148 \pm 17$   $CP$  odd events for  $B^\pm \rightarrow D_{CP}^0 K^\pm$  and  $37.6 \pm 7.4$   $CP$  even and  $14.8 \pm 5.9$   $CP$  odd states for  $B^\pm \rightarrow D_{CP}^0 K^{*\pm}$ . The results for  $r_B^2$  from these analysis are  $-0.12 \pm 0.08(\text{stat}) \pm 0.03(\text{syst})$  for  $B^\pm \rightarrow D_{CP}^0 K^\pm$  and  $0.30 \pm 0.25$  for  $B^\pm \rightarrow D_{CP}^0 K^{*\pm}$ . Thus far the GLW analyses do not tightly constrain  $r_B$  and more statistics are needed.

Table 1: *Measured ratios  $A_{CP\pm}$  and  $R_{CP\pm}$  for  $CP$ -even and  $CP$ -odd  $D$  decay modes. The first error is statistical and the second is systematic.*

	$B^\pm \rightarrow D_{CP}^0 K^\pm$	$B^\pm \rightarrow D_{CP}^0 K^{*\pm}$
$A_{CP+}$	$0.35 \pm 0.13 \pm 0.04$	$-0.08 \pm 0.19 \pm 0.08$
$A_{CP-}$	$-0.06 \pm 0.13 \pm 0.04$	$-0.26 \pm 0.40 \pm 0.12$
$R_{CP+}$	$0.90 \pm 0.12 \pm 0.04$	$1.96 \pm 0.40 \pm 0.11$
$R_{CP-}$	$0.86 \pm 0.10 \pm 0.05$	$0.65 \pm 0.26 \pm 0.08$

## 2.2 $\gamma$ from the Atwood-Dunietz-Soni Method

The ADS method is similar to the GLW method, except that it utilizes doubly Cabibbo-suppressed (DCS) decays rather than  $CP$  eigenstates. For the GLW method,  $CP$  asymmetries tend to be small because of the CKM and color suppression between the two interfering modes. In the ADS method, the  $CP$  violating effects can be enhanced when the final states are chosen to balance CKM and color suppression factors. For instance, the decays can be selected such that the color-favored  $B$  decay subsequently decays through a DCS  $D$  decay, and the color-suppressed  $B$  decay subsequently decays through a relatively CKM-favored  $D$  decay. However, the branching fractions for the DCS decays are small, and this method suffers from low yields. The  $D$  mode chosen for the analyses presented here is  $D^0 \rightarrow K^+ \pi^-$ .

For the ADS method, the observables are:

$$R_{ADS} = \frac{\Gamma(B^- \rightarrow [K^+ \pi^-]_D K^{(*)-}) + \Gamma(B^+ \rightarrow [K^- \pi^+]_D K^{(*)+})}{\Gamma(B^- \rightarrow [K^- \pi^+]_D K^{(*)-}) + \Gamma(B^+ \rightarrow [K^+ \pi^-]_D K^{(*)+})} \quad (5)$$

$$A_{ADS} = \frac{\Gamma(B^- \rightarrow [K^+ \pi^-]_D K^{(*)-}) - \Gamma(B^+ \rightarrow [K^- \pi^+]_D K^{(*)+})}{\Gamma(B^- \rightarrow [K^+ \pi^-]_D K^{(*)-}) + \Gamma(B^+ \rightarrow [K^- \pi^+]_D K^{(*)+})} \quad (6)$$

As in the GLW method, neglecting  $D^0 - \bar{D}^0$  mixing <sup>7)</sup>,  $R_{ADS}$  and  $A_{ADS}$  can be related to  $\gamma$ , the strong phases for the  $B$  and  $D$  decays,  $\delta_B$  and  $\delta_D$ , and the ratios of the suppressed-to-favored modes for the  $B$  and  $D$  decays,  $r_B$  and  $r_D$ :

$$R_{ADS} = r_D^2 + r_B^2 + 2r_D r_B \cos(\delta_B + \delta_D) \cos \gamma \quad (7)$$

$$A_{ADS} = 2r_D r_B \sin(\delta_B + \delta_D) \sin \gamma / R. \quad (8)$$

The CKM suppression factor for the  $D$  decay,  $r_D \equiv \frac{|A(D^0 \rightarrow K^+ \pi^-)|}{|A(D^0 \rightarrow K^- \pi^+)|}$ , is constrained to the experimental value of  $0.060 \pm 0.003$  <sup>10)</sup>.  $r_B$  and  $\delta_B$  can be

Table 2: Results for  $R_{ADS}$  and  $r_B$  for  $B^\mp \rightarrow \tilde{D}^0 K^\mp$  and  $B^\mp \rightarrow \tilde{D}^{*0} K^\mp$ . The first error is statistical and the second is systematic.  $r_B$  for  $B^\mp \rightarrow \tilde{D}^0 K^{*\mp}$  arises from combining the ADS and GLW results.

	$B^\mp \rightarrow \tilde{D}^0 K^\mp$	$B^\mp \rightarrow \tilde{D}^{*0} K^\mp$	$B^\mp \rightarrow \tilde{D}^{*0} K^\mp$	$B^\mp \rightarrow \tilde{D}^0 K^{*\mp}$
		$\tilde{D}^{*0} \rightarrow \tilde{D}^0 \pi^0$	$\tilde{D}^{*0} \rightarrow \tilde{D}^0 \gamma$	
$R_{ADS}$	$0.013^{+0.011}_{-0.009}$	$-0.002^{+0.010}_{-0.006}$	$0.011^{+0.018}_{-0.013}$	$0.046 \pm 0.031 \pm 0.008$
$R_{ADS}$ 90% C.L.	$< 0.029$	$< 0.023$	$< 0.045$	-
$r_B$	-		$0.004^{+0.014}_{-0.008}$	$0.28^{+0.06}_{-0.10}$
$r_B$ 90% C.L.	$< 0.23$		-	-
$r_B^{*2}$ 90% C.L.	-		$< (0.16)^2$	-

constrained to the values from the GLW analyses, leaving two unknowns,  $\delta_D$  and  $\gamma$ , and two measurable observables in the ADS analysis.

The latest ADS results from *BABAR* are based on 232 million  $B\bar{B}$  events (11), (12). The analyses reconstruct  $5^{+4}_{-3}$ ,  $-0.2^{+1.3}_{-0.7}$ ,  $1.2^{+2.1}_{-1.4}$ , and  $4.2 \pm 2.8$  signal events for  $\tilde{D}^0 K^-$ ,  $\tilde{D}^{*0}(\tilde{D}^0 \pi^0) K^-$ ,  $\tilde{D}^{*0}(\tilde{D}^0 \pi^0) K^-$ , and  $\tilde{D}^0 K^{*-}(K_S \pi^-)$  modes, respectively. No significant signal is observed in any of the channels studied. The results for  $R_{ADS}$  and  $r_B$  are shown in Table 2. For the  $B \rightarrow \tilde{D}^0 K$  channel, a limit on  $r_B$  is placed by allowing any value for  $\delta_D$  and  $\gamma$  and a  $1\sigma$  variation of  $r_D$ . The  $r_B$  result for  $B \rightarrow \tilde{D}^0 K^*$  comes from combining the results for the ADS and GLW methods. This combined result for  $B \rightarrow \tilde{D}^0 K^*$  also excludes the interval  $75^\circ \leq \gamma \leq 105^\circ$  at the  $2\sigma$  level. As in the case of the GLW analyses, more statistics are needed to put strong constraints on  $r_B$ .

### 2.3 $\gamma$ from the Giri-Grossman-Soffer-Zupan Dalitz Method

The GGSZ method utilizes  $D$  decays into three-body final states. Since the  $D$  can access the three-body final state through a number of resonances, a Dalitz analysis is done to fit the  $D^0 - \bar{D}^0$  interference region in the Dalitz plot and extract the desired  $CP$  parameters. One of the main advantages of this method is that by using a Dalitz fit, we can use the entire resonant structure of the three-body decay, including not only DCS decays, but also CKM-allowed decays as well as decays into  $CP$  eigenstates, thereby increasing our sensitivity to  $\gamma$ . The analysis presented here uses the common final state  $K_S \pi^+ \pi^-$ , employing  $K^0 - \bar{K}^0$  mixing in order to attain the same final state needed for interference.

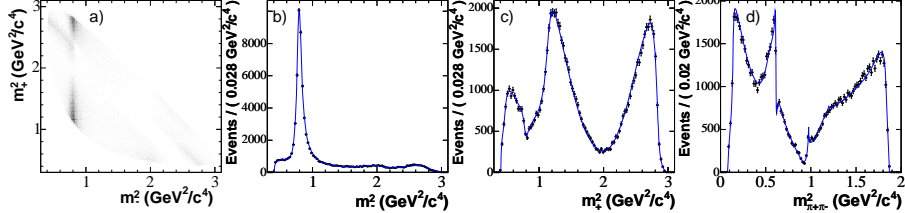


Figure 2: (a) The  $D^0 \rightarrow K_S \pi^- \pi^+$  Dalitz distribution from  $D^{*+} \rightarrow D^0 \pi^+$  events, and K-matrix model fit projections on (b)  $m_-^2$ , (c)  $m_+^2$ , and (d)  $m_{\pi^+ \pi^-}^2$ .  $\bar{D}^0 \rightarrow K_S \pi^+ \pi^-$  from  $D^{*-} \rightarrow \bar{D}^0 \pi^-$  events are also included.

The decay amplitude for  $B^\mp \rightarrow \tilde{D}^{(*)0} K^\mp$  can be expressed as:

$$A_\mp^{(*)}(m_\mp^2, m_\pm^2) = A_D(m_\mp^2, m_\pm^2) + r_B^{(*)} e^{i(\delta_B^{(*)} \mp \gamma)} A_D(m_\pm^2, m_\mp^2) \quad (9)$$

where  $m_-^2$  and  $m_+^2$  are the squared invariant masses  $K_S \pi^-$  and  $K_S \pi^+$ , respectively, and  $A_D$  is the  $D$  decay amplitude.

The current data sample of  $B \rightarrow \tilde{D}^{(*)0} K^{(*)}$  decays does not provide enough statistics to constrain  $A_D$ , which depends on the strong phase  $\delta_D$  and ratio of amplitudes  $r_D$ , in addition to  $\delta_B$ ,  $r_B$  and  $\gamma$ . A high statistics sample of flavor tagged  $D^0$  mesons from inclusive  $D^{*0} \rightarrow D^0 \pi^+$  decays is used to determine the  $D^0$  decay amplitude. A fit model must be chosen when parametrizing the  $D^0$  decay amplitude. The  $B \rightarrow \tilde{D}^{(*)0} K$  analysis uses a Breit-Wigner model, which includes 13 relativistic Breit-Wigner resonances and one non-resonant term. This model has proved inadequate at describing  $\pi\pi$  S-wave states, relying on the addition of  $\sigma(500)$  and  $\sigma'(1000)$  resonances, which are not well established, to improve the fit. A more accurate model based on the K-matrix formalism<sup>14), 15)</sup> and better suited for describing broad-overlapping resonances is used for the  $B \rightarrow \tilde{D}^0 K^*$  analysis. Figure 2 shows the Dalitz distribution from the  $D^{*+} \rightarrow D^0 \pi^+$  sample and the projections from the fit.

Once the  $D^0$  decay amplitude is determined, a simultaneous fit to the  $|A_-^{(*)}(m_-^2, m_+^2)|^2$  and  $|A_+^{(*)}(m_-^2, m_+^2)|^2$  distributions in the  $B^\mp \rightarrow \tilde{D}^0 K^\mp$  samples is used to extract  $r_B^{(*)}$ ,  $\delta_B^{(*)}$ , and  $\gamma$ . Using a sample of 227 million  $B\bar{B}$  events,  $282 \pm 20$ ,  $90 \pm 11$ ,  $44 \pm 8$ , and  $42 \pm 8$  signal  $\tilde{D}^0 K^-$ ,  $\tilde{D}^{*0}(\tilde{D}^0 \pi^0) K^-$ ,  $\tilde{D}^{*0}(\tilde{D}^0 \gamma) K^-$ , and  $\tilde{D}^0 K^{*-}(K_S \pi^-)$  events are reconstructed, respectively<sup>13), 16)</sup>. Figure 3 shows the contour projections of the constraint regions for  $r_B$  and  $\gamma$ . For  $B^- \rightarrow \tilde{D}^0 K^{*-}$ , a factor  $\kappa$  is introduced to take into account the contamination from  $B^- \rightarrow \tilde{D}^0(K_S \pi^-)_{non-K^*}$  decays. There is two-fold ambiguity on  $\gamma$

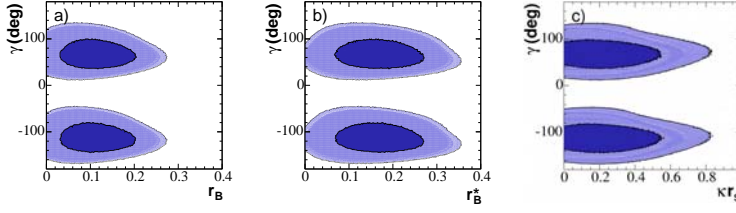


Figure 3: Two-dimensional projections onto the (a)  $r_B - \gamma$ , (b)  $r_B^{(*)} - \gamma$ , and (c)  $\kappa r_s - \gamma$  planes of the seven-dimensional one- (dark) and two- (light) standard deviation regions, for the combination of  $B^- \rightarrow \tilde{D}^{*0} K^-$  and  $B^- \rightarrow \tilde{D}^0 K^{*-}$ .

from this method. Combining the three modes results in  $\gamma = (67 \pm 28(\text{stat}) \pm 13(\text{syst}) \pm 11(\text{model}))^\circ$ , where the third error is due to the uncertainty in the Dalitz fit model.

### 3 $\sin(2\beta + \gamma)$ from $B^0 \rightarrow D\pi$ , $B^0 \rightarrow D^*\pi$ , and $B^0 \rightarrow D\rho$ Decays

The results presented thus far in this paper rely on time-independent methods for extracting  $\gamma$ . The study of time-dependent asymmetries in neutral  $B$  decays  $B^0 \rightarrow D^{(*)}\pi$  and  $B^0 \rightarrow D\rho$  can also be used to measure  $\sin(2\beta + \gamma)$ , and hence  $\gamma$ . Like the analyses described earlier, this method studies the interference between CKM-suppressed  $b \rightarrow u$  and CKM-favored  $b \rightarrow c$  transitions, which have a relative weak phase of  $\gamma$ . In the time-dependent study there is an additional weak phase of  $2\beta$  from  $B^0 - \bar{B}^0$  mixing. The dominant Feynman diagrams for the CKM-favored decay  $B^0 \rightarrow D^-\pi^+$  and the doubly CKM-suppressed decay  $B^0 \rightarrow D^+\pi^-$  can be seen in Figure 4. The ratio between suppressed and favored decays is estimated to be  $\sim 0.02$ , and thus, the  $CP$  violating effects are expected to be small using this method.

The expression for time-dependent decay rate for the  $B^0$  decaying to final state  $\mu = D\pi, D^*\pi, D\rho$ , neglecting the decay width difference, is:

$$f^{\pm,\mu}(\eta, \Delta t) = \frac{e^{-|\Delta t|/\tau}}{4\tau} \times [1 \mp (a^\mu \mp \eta b - \eta c^\mu) \sin(\Delta m_d \Delta t) \mp \eta \cos(\Delta m_d \Delta t)] \quad (10)$$

where  $\tau$  is the  $B^0$  lifetime,  $\Delta m_d$  is the  $B^0 - \bar{B}^0$  mixing frequency, and  $\Delta t$  is the time difference between the  $B^0 \rightarrow D^{(*)\pm}\pi^\mp$  or  $B^0 \rightarrow D^\pm\rho^\pm$  decay ( $B_{rec}$ ) and the decay of the other  $B$  from the  $\Upsilon(4S)$  decay ( $B_{tag}$ ). The upper (lower) sign refers to the flavor of the tagged  $B$  as  $B^0$  ( $\bar{B}^0$ ), while  $\eta = +1(-1)$  for the

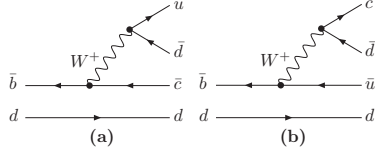


Figure 4: Feynman diagrams for (a) the CKM-favored decay  $B^0 \rightarrow D^- \pi^+$  and (b) the doubly CKM-suppressed decay  $B^0 \rightarrow D^+ \pi^-$

final state with a  $D^{(*)-}(D^{(*)+})$ .  $a^\mu$ ,  $b$  and  $c^\mu$  can be written in terms of the  $CP$  parameters  $r^\mu$ ,  $\delta^\mu$ , and  $2\beta + \gamma$  as:

$$a^\mu = 2r^\mu \sin(2\beta + \gamma) \cos \delta^\mu \quad (11)$$

$$b = 2r' \sin(2\beta + \gamma) \cos \delta' \quad (12)$$

$$c^\mu = 2 \cos(2\beta + \gamma) (r^\mu \sin \delta^\mu - r' \sin \delta'). \quad (13)$$

The parameters  $r'$  and  $\delta'$  account for the non-negligible  $CP$  violating effects on the tagged side of the decay. Only  $c^\mu$  from events tagged with leptons, which have do not suffer from such tag-side interference, and  $a^\mu$  are used in determining  $\sin(2\beta + \gamma)$ .

Since our experimental sensitivity is limited by the small size of  $r^\mu$ , it is not possible to extract  $\sin(2\beta + \gamma)$ ,  $\delta^\mu$  and  $r^\mu$  from the available dataset. External input for  $r^\mu$  is therefore needed. A measurement of the branching fractions for the the favored and suppressed modes would give us the required input, but unfortunately, the direct measurement of the branching fractions for the doubly CKM-suppressed modes are not possible because of the overwhelming background from the favored mode. However, assuming SU(3) flavor symmetry,  $r^\mu$  can be related to the branching ratios for  $B^0 \rightarrow D_s^{(*)+} \pi^-$  or  $B^0 \rightarrow D_s^+ \rho^-$ , the measurements for which are more experimentally feasible 17), 18).

Full and partial reconstruction methods are used for studying  $B^0 \rightarrow D^{*-} \pi^+$  decays. In the full reconstruction method, the decay chain is fully reconstructed, which results in a high signal purity, but low efficiency. In the partial reconstruction method, only the daughter pion of the  $B^0$  and the slow pion from  $D^{*-} \rightarrow D^0 \pi^-$  decays are reconstructed, which results in a high efficiency but also a high level of backgrounds.

The results from *BABAR* using 232 million  $B\bar{B}$  events, from both the full and partial reconstruction methods, are shown in Table 3 19), 20). The

Table 3: Results for  $CP$  parameters  $a^\mu$  and  $c_{lepton}^\mu$  for  $B^0 \rightarrow D^{(*)}\pi$  and  $B^0 \rightarrow D\rho$  from full and partial reconstruction methods.

mode	$a^\mu$	$c_{lepton}^\mu$
$B^0 \rightarrow D\pi$ (full reco)	$-0.010 \pm 0.023 \pm 0.007$	$-0.033 \pm 0.042 \pm 0.012$
$B^0 \rightarrow D^*\pi$ (full reco)	$-0.040 \pm 0.023 \pm 0.010$	$0.049 \pm 0.042 \pm 0.015$
$B^0 \rightarrow D\rho$ (full reco)	$-0.024 \pm 0.031 \pm 0.009$	$-0.098 \pm 0.055 \pm 0.018$
$B^0 \rightarrow D^*\pi$ (partial reco)	$-0.034 \pm 0.014 \pm 0.009$	$-0.019 \pm 0.022 \pm 0.013$

signal yields from the full reconstruction method are  $15038 \pm 132$ ,  $14002 \pm 123$ ,  $8736 \pm 101$  events for  $D\pi$ ,  $D^*\pi$ , and  $D\rho$ , respectively. The signal yields from the partial reconstruction method for  $D^*\pi$  are  $18710 \pm 270$  events in the lepton-tag category and  $70580 \pm 660$  events in the kaon-tag category. The resulting lower limits on  $|\sin(2\beta + \gamma)|$  at the 68% (90%) C.L. are  $|\sin(2\beta + \gamma)| > 0.64$  (0.40) for  $D^{(*)}\pi$  and  $D\rho$  from the full reconstruction method, and  $|\sin(2\beta + \gamma)| > 0.62$  (0.35) for  $D^*\pi$  from the partial reconstruction method.

#### 4 Conclusions

Although direct measurement of  $\gamma$  was impossible at the  $B$ -factories a few years ago, much progress has been made and it is now an important and significant part of constraining the Unitarity Triangle. The errors on  $\gamma$  are still statistically limited, but as *BABAR* collects more data, with an expected  $1 \text{ ab}^{-1}$  by 2008, the error on  $\gamma$  is estimated to decrease to less than  $10^\circ$ . We are now entering a phase when the direct measurement of the angles of the Unitarity Triangle can determine  $(\rho, \eta)$  at a comparable precision as all data combined.

#### 5 Acknowledgements

I would like to thank my *BABAR* and PEP-II colleagues whose expertise and dedication made these results possible. This work was supported in part by U.S. Department of Energy contract DE-AC02-76SF00515.

#### References

1. N. Cabibbo, Phys. Rev. Lett. **10**, 531 (1963); M. Kobayashi and T. Maskawa, Prog. Theor. Phys. **49**, 652 (1973).

2. C. Jarlskog, in *CP Violation*, C. Jarlskog ed., World Scientific, Singapore (1988).
3. M. Gronau, Phys. Lett. **B557**, 198 (2003).
4. M. Gronau, D. London, Phys. Lett. B **253**, 483 (1991); M. Gronau, D. Wyler, Phys. Lett. B **265**, 172 (1991).
5. D. Atwood, I. Dunietz, A. Soni, Phys. Rev. Lett. **78**, 3257 (1997); Phys. Rev. D **70**, 091503 (2004).
6. A. Giri, Y. Grossman, A. Soffer, and J. Zupan, Phys. Rev. D **68**, 054018 (2003).
7. Y. Grossman, A. Soffer, J. Zupan, Phys. Rev. **D72**, 031501 (2005).
8. *BABAR* Collaboration, B. Aubert *et al.*, Phys. Rev. **D73** 051105 (2006).
9. *BABAR* Collaboration, B. Aubert *et al.*, Phys. Rev. **D72** 071103 (2005).
10. *BABAR* Collaboration, B. Aubert *et al.*, Phys. Rev. Lett. **91**, 171801 (2003).
11. *BABAR* Collaboration, B. Aubert *et al.*, Phys. Rev. **D72**, 032004 (2005).
12. *BABAR* Collaboration, B. Aubert *et al.*, Phys. Rev. **D72**, 071104 (2005).
13. *BABAR* Collaboration, B. Aubert *et al.*, Phys. Rev. Lett. **95**, 121802 (2005).
14. E. P. Wigner, Phys. Rev. 70 (1946) 15; S. U. Chung *et al.*, Ann. Physik 4 (1995) 404.
15. I. J. R. Aitchison, Nucl. Phys. **A189**, 417 (1972).
16. hep-ex/0507101
17. I. Dunietz, Phys. Lett. **B427**, 179 (1998).
18. hep-ex/0604012
19. hep-ex/0602049
20. *BABAR* Collaboration, B. Aubert *et al.*, Phys. Rev. **D71**, 112003 (2005).